Pergamon

Geochimica et Cosmochimica Acta, Vol. 68, No. 22, pp. 4665-4678, 2004

0016-7037/04 $30.00 + .00

doi:10.1016/j.gca.2004.05.029

Rate-controlled calcium isotope fractionation in synthetic calcite

D. LEMARCHAND,[1,*,†] G. J. WASSERBURG,[1] and D. A. PAPANASTASSIOU[1,2]

[1]The Lunatic Asylum, Division of Geological and Planetary Sciences, California Institute of Technology, Pasadena, CA 91125, USA
[2]Earth and Space Sciences Division, Mail Stop 183-335, Jet Propulsion Laboratory, California Institute of Technology, 4800 Oak Grove Drive, Pasadena, CA 91109-8099 USA

(*Received February* 11, 2004; *accepted in revised form May* 26, 2004)

Abstract—The isotopic composition of Ca ($\Delta^{44}Ca/^{40}Ca$) in calcite crystals has been determined relative to that in the parent solutions by TIMS using a double spike. Solutions were exposed to an atmosphere of NH_3 and CO_2, provided by the decomposition of $(NH_4)_2CO_3$, following the procedure developed by previous workers. Alkalinity, pH and concentrations of CO_3^{2-}, HCO_3^-, and CO_2 in solution were determined. The procedures permitted us to determine $\Delta(^{44}Ca/^{40}Ca)$ over a range of pH conditions, with the associated ranges of alkalinity. Two solutions with greatly different Ca concentrations were used, but, in all cases, the condition $[Ca^{2+}]>>[CO_3^{2-}]$ was met. A wide range in $\Delta(^{44}Ca/^{40}Ca)$ was found for the calcite crystals, extending from $0.04 \pm 0.13‰$ to $-1.34 \pm 0.15‰$, generally anti-correlating with the amount of Ca removed from the solution. The results show that $\Delta(^{44}Ca/^{40}Ca)$ is a linear function of the saturation state of the solution with respect to calcite (Ω). The two parameters are very well correlated over a wide range in Ω for each solution with a given [Ca]. The linear correlation extended from $\Delta(^{44}Ca/^{40}Ca) = -1.34 \pm 0.15‰$ to $0.04 \pm 0.13‰$, with the slopes directly dependent on [Ca]. Solutions, which were vigorously stirred, showed a much smaller range in $\Delta(^{44}Ca/^{40}Ca)$ and gave values of $-0.42 \pm 0.14‰$, with the largest effect at low Ω. It is concluded that the diffusive flow of CO_3^{2-} into the immediate neighborhood of the crystal-solution interface is the rate-controlling mechanism and that diffusive transport of Ca^{2+} is not a significant factor. The data are simply explained by the assumptions that: a) the immediate interface of the crystal and the solution is at equilibrium with $\Delta(^{44}Ca/^{40}Ca) \sim -1.5 \pm 0.25‰$; and b) diffusive inflow of CO_3^{2-} causes supersaturation, thus precipitating Ca from the regions exterior to the narrow zone of equilibrium. The result is that $\Delta(^{44}Ca/^{40}Ca)$ is a monotonically increasing (from negative values to zero) function of Ω. We consider this model to be a plausible explanation of most of the available data reported in the literature. The well-resolved but small and regular isotope fractionation shifts in Ca are thus not related to the diffusion of very large hydrated Ca complexes, but rather due to the ready availability of Ca in the general neighborhood of the crystal-solution interface. The largest isotopic shift which occurs as a small equilibrium effect is then subdued by supersaturation precipitation for solutions where $[Ca^{2+}]>>[CO_3^{2-}] + [HCO_3^-]$. It is shown that there is a clear temperature dependence of the net isotopic shifts that is simply due to changes in Ω due to the equilibrium "constants" dependence on temperature, which changes the degree of saturation and hence the amount of isotopically unequilibrated Ca precipitated. The effects that are found in natural samples, therefore, will be dependent on the degree of diffusive inflow of carbonate species at or around the crystal-liquid interface in the particular precipitating system, thus limiting the equilibrium effect.

1. INTRODUCTION

The purpose of this work was to carry out experiments to understand the calcium isotopic fractionation that takes place during the growth of calcite from solution. It is well known that calcium isotopic shifts occur in natural marine carbonate samples (calcite and aragonite) relative to seawater (Zhu and Macdougall, 1998; Halicz et al., 1999; De La Rocha and DePaolo, 2000; Nägler et al., 2000; Schmitt et al., 2003). It has further been suggested that this may be used as a thermometer. Recent experiments have shown clear fractionation effects due to kinetic isotopic effects on Ca isotopic abundances relative to the parent solution for aragonite grown under laboratory conditions (Gussone et al., 2003). The growth of calcite and aragonite has been an area of intense study by many workers for decades due to the important role of CO_2 and carbonate dissolution/precipitation in the oceans and the general connections to climate. There are several studies reporting on Ca isotopic fractionation in biologic systems and reports of fractionation in the growth of foraminifera (Skulan et al., 1997; Zhu and Macdougall, 1998; Nägler et al., 2000; Gussone et al., 2003). This study focuses on Ca fractionation produced in a laboratory study of a simple inorganic system. There should be some connection between the results found here and those involved in complex organic processes, but these issues are not in general addressed here. We consider that biologic systems will produce isotopic fractionation by normal physical-chemical laws. The key questions in biologic systems are the reaction pathways and the number of reaction stages that are used to precipitate $CaCO_3$ (aragonite or calcite). The actual mechanisms used by different organisms in precipitating $CaCO_3$ are not well established and remain an area of investigation.

There have been extensive laboratory studies relating to isotopic shifts in carbon and in oxygen in carbonate-aqueous solutions to understand the basic chemical kinetic-equilibrium

* Author to whom correspondence should be addressed (lemarcha@illite.u-strasbg.fr).
† *Current address:* École et Observatoire des Sciences de la Terre, Centre de Géochimie de la Surface, 1 rue Blessig-67084 Strasbourg Cedex, France.

problems involved in paleothermometry (e.g., Botttinga, 1968; Turner, 1982; Grossman and Ku, 1986; McConnaughey, 1988; Romanek et al., 1991; Kim and O'Neil, 1997; Zeebe, 1999; Jiménez-Lopez et al., 2001). These studies have demonstrated the complex role of the various species of carbon involved in the reactions, including at the crystal-liquid interface. Extensive studies on the kinetics of both the forward and backward reactions in calcite growth from solution have laid out the fundamental rules for mechanisms and rates of precipitation of carbonates/calcite from solution (e.g., Plummer et al., 1978; Plummer and Busenberg, 1982; Mucci, 1983; Nielsen, 1984; Nielsen and Toft, 1984; Zuddas and Mucci, 1994a, 1994b). Both of these types of studies demonstrate that the concentrations of carbonate species are the governing parameters in this crystal growth process, particularly when the condition $[Ca^{2+}]>>[CO_3^{2-}]$ is met.

In the present study we carried out a series of experiments on calcite precipitation from solutions supersaturated at different levels with respect to calcite by varying Ca^{2+} and CO_3^{2-} concentrations. These changes induced different calcite precipitation rates, using both purely diffusion-limited growth and growth from stirred solutions. It is well known that, while there is a large fractional mass difference (10%) between ^{44}Ca and ^{40}Ca, the isotopic shifts are very small (typically less than 0.4 ‰/amu). The double spike technique was used in the present study following the first work by Russell et al. (1978) who established the levels of Ca isotopic fractionation in nature and the methodology for obtaining reliable data.

The experiment was designed to test the degree of isotopic fractionation that occurred in calcite crystals as a function of the amount of calcite removed from solution. It was considered that kinetic effects due solely to diffusive Ca transport from solution would show the largest isotopic shifts for the smallest fractional amount of Ca removed from solution. The fractional amounts removed ranged from 10^{-2}% to 10% of the total Ca in solution. The degree to which the isotopic shifts for any experiment were uniform as a function of position in the container and were the same on a macroscopic and microscopic scale was studied. A range of precipitation rates was investigated. Two solutions were used with a factor of ten difference in Ca concentrations to establish whether the Ca concentration affected the results. In addition, the chemical state of the solutions was measured with particular regard to determining the degree of saturation of the solutions during crystal growth. The conditions that previous workers had studied, which controlled C and O isotopic fractionation, were used as a guide in considering the results, but no effort was made to measure the C and O in the samples.

2. ANALYTICAL PROCEDURES

2.1. Crystal Growth Method

Synthetic calcite crystals were grown following the procedure first developed by Gruzensky (1967) and later used in studies concerned with calcite and aragonite growth mechanisms and incorporation of trace elements into calcium carbonates (e.g., Paquette and Reeder, 1990; Hemming et al., 1995). This method allows individual calcite crystals to precipitate from solution in a sealed volume, where the gases from decomposition of solid ammonium carbonate $(NH_4)_2CO_3$ interact with a $CaCl_2$-NH_4Cl solution (see Fig. 1). At ambient temperature, ammonium carbonate crystals decompose according to the reaction:

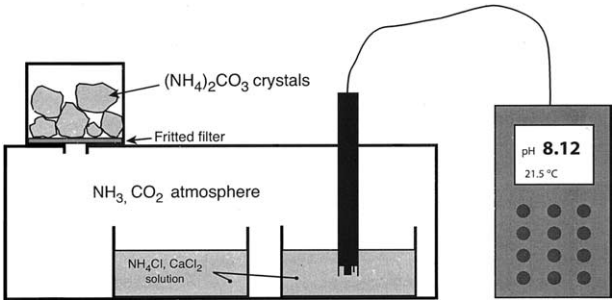

Fig. 1. Schematic illustration of the experimental calcite precipitation. Ammonium carbonate crystals decompose in a sealed volume yielding a CO_2/NH_3 rich atmosphere. This atmosphere further equilibrates with the $CaCl_2$-NH_4Cl solution to reach a supersaturation state with respect to calcite. After Gruzensky, 1967 and Hemming et al. (1995).

$$(NH_4)_2CO_3 \Rightarrow 2NH_{3(g)} + CO_{2(g)} + H_2O_{(g)} \quad (1)$$

Gaseous species NH_3 and CO_2 dissolve and diffuse into the $CaCl_2$-NH_4Cl solution in which they dissociate following the equilibrium reaction schemes:

$$NH_{3(g)} \leftrightarrow NH_{3(aq)} \quad (2)$$

$$NH_{3(aq)} + H_2O \overset{K^*_{NH_3}}{\leftrightarrow} NH_4^+ + OH^- \quad (3)$$

$$CO_{2(g)} \leftrightarrow CO_{2(aq)} \quad (4)$$

$$CO_{2(aq)} + H_2O \leftrightarrow H_2CO_3 \quad (5)$$

$$H_2CO_3 \overset{K_1^*}{\leftrightarrow} HCO_3^- + H^+ \quad (6)$$

$$HCO_3^- \overset{K_2^*}{\leftrightarrow} CO_3^{2-} + H^+ \quad (7)$$

where K* denote apparent dissociation constants in solution and depend on the temperature and salinity of the solution. These reactions result in an increase of the total alkalinity and pH of the solution yielding an increase in the supersaturation conditions with respect to calcite (Ω) as defined below:

$$\Omega = \frac{[Ca^{2+}] \times [CO_3^{2-}]}{K^*_{sp}} \quad (8)$$

where K^*_{sp} is the solubility product of calcite in the experimental solution. We recognize that there are both forward and back reactions and that the rate constants and equilibrium constants are actually apparent values dependent on the nature of the solutions, in the sense described by Zuddas and Mucci (1994a) in their thorough study of the reaction paths. The values of K* used in this work are discussed in Section 3.2.

The system NH_3/NH_4^+ buffers the pH during calcite precipitation experiments. After a short transitional period, during which the solid/atm/solution system equilibrates, the solution reaches a state characterized by a quasi-constant pH value during calcite-precipitation.

2.2. Materials and Experimental Setup

Two separate $CaCl_2$-NH_4Cl solutions were prepared: solution #A has [Ca] = 150 mmol/L and solution #B has [Ca] = 15 mmol/L. Both solutions initially have $[NH_4]$ = 0.395 mol/L. The ionic strengths and Ca isotopic compositions are reported in Table 1. All experiments were carried out at room temperature, T = 21 ± 1 °C. Two polypropylene beakers, each containing ~150 mL of the $CaCl_2$-NH_4Cl solution, were placed inside a 4.8 L plastic container, which was then sealed. The depth of the solution in each beaker was 3 cm. One of the solutions in the beakers was used to monitor pH and temperature during the course

Table 1. Chemical composition and δ^{44} Ca analyses of the $CaCl_2$-NH_4Cl solutions

Sol. #	[$CaCl_2$] (mmol/l)	[NH_4Cl] initial (mmol/l)	Salinity (‰)	Ionic Strength (mol/l)	$\Delta\ ^{44}Ca$[§] (‰) ± 2σ
A	150	395	37.8	0.85	0.05 ± 0.17
A	150	395	37.8	0.85	0.18 ± 0.14
A	150	395	37.8	0.85	0.16 ± 0.09
A	150	395	37.8	0.85	0.12 ± 0.15
				mean	0.13
B	15	395	22.7	0.45	0.14 ± 0.14
B	15	395	22.7	0.45	0.09 ± 0.12
				mean	0.12
				Grand mean	0.12 ± 0.04

[§] The isotopic compositions are expressed as the deviations from the CaF_2 standard solution: $^{42}Ca/^{40}Ca = 0.00662$; $^{44}Ca/^{40}Ca = 0.02121$; $^{48}/Ca/^{40}Ca = 0.001881$, after Russell et al. (1978). The isotopic ratios of the ^{42}Ca-^{48}Ca spike are $^{42}Ca/^{40}Ca = 15.976$; $^{44}Ca/^{40}Ca = 0.14684$; $^{48}Ca/^{40}Ca = 4.604$. Separated isotopes (as $^{42}CaCo_3$, $^{48}CaCO_3$) were obtained from ORNL.

of calcite precipitation; the other solution beaker was used to collect the accumulated calcite crystals. A typical mass of 5–10 g of ammonium carbonate (crystal size ~1 cm) was placed in a separate vessel connected to the plastic housing container through a fritted filter (see Fig. 1). After a precipitation experiment was completed, the solution was gently drained to keep in place the calcite crystals, which had grown on the vessel walls. The vessel, still holding the attached crystals, was then rinsed three times with de-ionized water and dried.

To test the influence of different parameters on the Ca isotopes, crystals were grown under various experimental conditions: two different calcium concentrations, various pH values, from stagnant solutions and from solutions stirred with a magnetic stirrer at 300 rpm.

2.3. Sample Preparation and Calcium Isotope Determination

Calcite crystals were dissolved in HCl, 3N. The isotopic ratios were determined by Thermal Ionization Mass Spectrometry (TIMS) on the Lunatic I (Wasserburg et al., 1969), using a double-spike technique. A ^{42}Ca-^{48}Ca enriched Ca solution (so-called "double-spike") of precisely known Ca isotopic ratios was added to an aliquot of the dissolved calcite solution to correct for isotopic fractionation occurring during the course of the analysis. A new ^{42}Ca-^{48}Ca double-spike solution was prepared by mixing weighed single isotope standard solutions (^{42}Ca and ^{48}Ca, provided by the Oak Ridge National Laboratory). The concentrations of the individual ^{42}Ca and ^{48}Ca spike solutions were determined by isotope dilution using the CaF_2 standard solution analyzed by (Russell et al. 1978). The ^{42}Ca and ^{48}Ca ($^{42,48}Ca$) tracer solutions were then mixed to obtain $^{42}Ca/^{48}Ca$ in the double-spike solution, which was approximately equal to the normal $^{42}Ca/^{48}Ca$ value. Aliquots of the ^{42}Ca-^{48}Ca double-spike solution were then calibrated by analyzing on the mass spectrometer, mixtures of the double tracer and the CaF_2 standard solution and using the $^{40}Ca/^{44}Ca = 47.153$ isotopic ratio of the CaF_2 standard solution as used by Russell et al. (1978). Thus, the calcium isotopic ratios given in the present study are consistent with those previously reported by the Lunatic Asylum as both studies use the same normalization for the same Ca standard solution. The calcium isotope abundances of the double-spike solution are reported in the footnote of Table 1. The spiked samples were dried under an ultraviolet lamp and the residue dissolved in 2 μL HNO_3. The latter solution was then loaded without any further treatment on a single, V-shaped, oxidized Ta filament.

First, an analysis was done on an aliquot of the dissolved calcite sample to determine the calcium concentration in the solution. Then, an aliquot corresponding to 5 μg of Ca was spiked and analyzed to precisely determine the isotopic composition. To control the quality of the data, the $^{40}Ca/^{42}Ca$ ratio in the spiked mixture was kept at 7 ± 1. Replicate analyses were done and are reported in the data table.

The filament was gradually preheated up to ~1200 °C, the temperature then adjusted to reach a typical beam of 4×10^{-11} A of $^{40}Ca^+$ at filament temperatures from 1370 to 1410°C. Data were then collected by sequentially stepping at mass 40, 42, 44 and 48 with systematic bracketing of background measurements. Mean isotopic ratios of $^{42}Ca/^{40}Ca$, $^{44}Ca/^{40}Ca$, $^{48}Ca/^{40}Ca$, and $^{48}Ca/^{42}Ca$ are calculated over 250–300 cycles. The final tabulated $^{44}Ca/^{40}Ca$ isotopic ratios represent the values corrected for instrumental fractionation using the average measured isotopic ratios coupled to the known values in the tracer to obtain the isotopic shifts using the mass discrimination law given by Russell et al. (1978).

The calcium isotopic compositions are expressed as the deviation from the value of the CaF_2 standard solution, using the δ notion (in ‰):

$$\delta^{44}Ca = \left[\frac{\left(^{44}Ca/^{40}Ca\right)_{sample}}{\left(^{44}Ca/^{40}Ca\right)_{standard}} - 1 \right] \times 10^3 \quad (9)$$

where $^{44}Ca/^{40}Ca_{standard}$ refers to the $^{44}Ca/^{40}Ca$ isotopic ratio of the CaF_2 standard solution analyzed by Russell et al. (1978). As we wish to compare the isotopic shifts of the calcite crystal grown with the values in the original parent solution, we use the representation:

$$\Delta^{44/40}Ca = \delta^{44}Ca_{crystals} - \delta^{44}Ca_{solution} \quad (10)$$

Separate analyses were done of the standard solution and of the growth solution as well as repeated analyses of the samples of the dissolved calcite produced in the experiments. The results show a typical in-run precision of 0.15‰ (± 2σ) and a long-term reproducibility of 0.12‰ (±2σ), see Tables 2 and 3.

3. RESULTS

3.1. Identification, Morphology and Crystal Size

After every precipitation experiment was completed, small quantities of calcite crystals were found attached to the beaker walls. No crystals were found in the mother solution upon decanting. Optical microscope observations showed typical calcite morphologies. It was found by scanning electron microscopy (SEM imaging) that all the crystals were well defined calcite rhombohedra. About 1/6 of the crystals showed one face with a somewhat undulating or smooth side that was not a rhombohedral face. Such faces can be seen in Figure 2a (crystals on top left and right side of the picture). These observations suggest that crystals had grown directly on the vessel walls rather than from the volume of the solution with later deposition on the vessel walls. Some samples were subjected to X-ray diffraction tests to establish that the phase was calcite. For most experiments, calcite was found to be the only phase to crystallize. However, in some cases, a second phase could be observed optically and was identified by X-ray diffraction as vaterite, a

Table 2. Summary and results of calcite precipitation experiments

Exp. #	Duration (h)	pH final	Alk. (meq/l)	Ca removed. (mg)	Ca removed. % of total	$\Delta\ ^{44}Ca$[§] (‰) ± 2σ	$[CO_3^{2-}]$[‡] (μmol/l)	Ω[‡]	Log(R)[‡]* (μmol/m^2/h)
[Ca] = 150 mmol/l in initial solution (#A)									
1	101	8.30	24.0	88	10	0.04 ± 0.13	339 ± 87	105 ± 23	4.7 ± 0.3
1			replicate			−0.03 ± 0.11			
2	76	8.04	13.0	9.2	1	−0.78 ± 0.13	103 ± 87	32 ± 8	2.9 ± 0.4
3	25	8.02	11.9	0.1	0.01	−1.12 ± 0.12	60 ± 26	19 ± 7	2.2 ± 0.5
3			replicate			−1.01 ± 0.14			
4	26	8.22	19.0	0.4	0.04	−0.72 ± 0.13	153 ± 60	48 ± 16	3.5 ± 0.5
5	25	8.00	11.1	0.06	0.01	−1.23 ± 0.17	38 ± 23	12 ± 6	1.5 ± 0.7
6	40	7.97	11.0	1.0	0.11	−0.87 ± 0.16	72 ± 22	22 ± 6	2.4 ± 0.4
6			replicate			−1.03 ± 0.11			
[Ca] = 15 mmol/l in initial solution (#B)									
7	27	8.40	28.9	3	4	−0.05 ± 0.13	351 ± 133	20 ± 3	4.7 ± 0.4
8	69	8.32	23.8	5	6	−0.56 ± 0.15	228 ± 96	13 ± 2	4.1 ± 0.3
8			replicate			−0.55 ± 0.13			
9	45	8.07	13.1	0.03	0.03	−1.34 ± 0.15	60 ± 33	3 ± 1	2.2 ± 0.06
10	91	8.21	19.6	3.2	4	−0.44 ± 0.13	259 ± 64	15 ± 2	4.3 ± 0.1
Stirred solutions (300 rpm)									
[Ca] = 150 mmol/l in initial solution (#A)									
11	39	8.12	16.7	44	5	−0.20 ± 0.12	230 ± 43	71 ± 11	4.1 ± 0.2
12	32	7.65	5.1	4.7	1	−0.42 ± 0.14	13 ± 5	4 ± 1	−0.1 ± 0.5
12			replicate			−0.36 ± 0.11			
13	35	7.96	11.0	18	2	−0.31 ± 0.15	84 ± 21	26 ± 5	2.6 ± 0.3
[Ca] = 15 mmol/l in initial solution (#B)									
14	46	8.09	15.2	4.0	4	−0.26 ± 0.14	185 ± 40	11 ± 1	3.8 ± 0.1
15	58	8.22	20.2	9.3	10	−0.20 ± 0.13	284 ± 67	16 ± 2	4.4 ± 0.1

All the precipitation experiments have been carried out at a constant temperature 21 ± 1 °C; and initial $[NH_4Cl]$ = 395 mmol/l.
§ Ca isotopic composition expressed as the difference from the mother solution = $\Delta^{44}Ca = \delta^{44}Ca_{crystals} - \delta^{44}Ca_{solution}$.
‡ Relative uncertainties on $[CO_3^{2-}]$, Ω and R. See text for discussion about absolute uncertainties.
* Precipitation rates are calculated from the empirical law determined by Zuddas and Mucci (1994), see text for details.

$CaCO_3$ polymorph. The presence of vaterite was then checked in all samples by optical microscopy and every experiment for which vaterite was detected was not analyzed.

Solutions which were not stirred yielded a sparse distribution of crystals on the beaker walls (~5–10 crystals/cm^2) with a typical size of ~100 μm after ~100 h of growth (see Fig. 2a). However, a slight difference in the density of calcite crystals per unit area is observed between the two solutions #A and #B. Solution #B ([Ca] = 15 mmol/L) yielded a rather uniform concentration of crystals grown both on the sides and the bottom of the beaker. The first crystals usually appeared 25–48 h after the experiment was initiated, depending on the supersaturation state of the solution. Calcite crystals appear to grow simultaneously on all the immersed surfaces of the vessel, reflecting a rather homogeneous chemical composition of the precipitating solution (in particular with respect to the CO_3^{2-} species). In contrast, the solution #A ([Ca] = 150 mmol/L) caused crystals to precipitate a bit earlier in the course of the experiment (typically, 24 h after the experiments were started) that led to the development of a crystallization front moving from the atmosphere/solution interface and reaching the bottom of the solution after 48–72 h. After 24 h of growth from solutions of #A, crystals covered the first centimeter of the vessel walls below the atmosphere/solution interface. After 72 h, calcite crystals were observed on the bottom of the beaker (3 cm below the solution surface). The propagation of the calcite precipitation front toward deeper layers of the solution reflects a stratification of the solution chemistry resulting from

Table 3. $\delta^{44}Ca$ of calcite crystals handpicked from the vessel walls

Sample. # (ref. Table 2)		Distance from solution top (mm)	[Ca] (mmol/l)	Mass of Ca in calcite (μg)	$\Delta^{44}Ca$ (‰) ± 2σ
From #2	Top	0	150	40	−0.84 ± 0.15
	Bottom	30	150	60	−0.68 ± 0.16
	Bottom		replicate		−0.88 ± 0.12
	Avg.Bulk		150	9200	−0.78 ± 0.13
From #10	Top	0	15	70	−0.32 ± 0.11
	Middle	10	15	100	−0.39 ± 0.12
	Bottom	25	15	80	−0.44 ± 0.12
	Avg. Bulk		15	3200	−0.44 ± 0.13

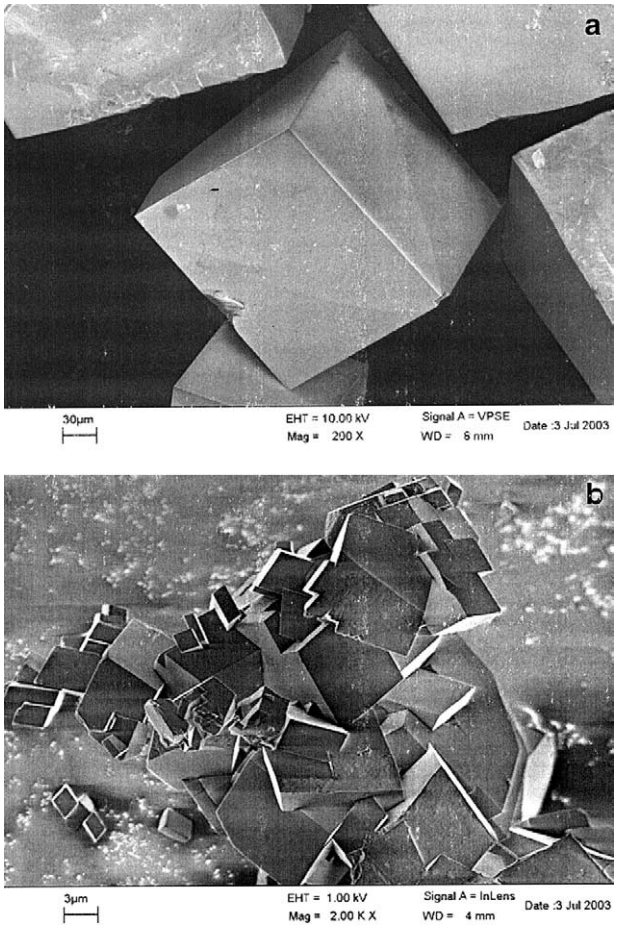

Fig. 2. Scanning electron microscope images of calcite crystals grown under various experimental conditions. a) the precipitating solution has remained unstirred. b) the precipitating solution has been stirred at 300 rpm. Note the scale difference.

the diffusion into the solution of carbon and nitrogen species from the CO_2-NH_3-rich atmosphere. The value of $[CO_3^{2-}]$ for saturation of solution #A is 0.003 mmol/L while it is 0.018 mmol/L for solution #B because of the effect of salinity dependence. This is a factor of 6 taking the ionic strength into account (see Sec. 3.2). Assuming that the carbonate species are transported in the solution layer only by diffusion, then the $[CO_3^{2-}]$ value required to initiate nucleation is less for higher [Ca] and thus occurs earlier in the course of the experiment. In this case, for solutions of #A, only the upper half of the solution had reached saturation conditions favorable to calcite nucleation after 24 h. For the lower [Ca] values of solution #B, the required $[CO_3^{2-}]$ is higher and is achieved later.

Some experiments were done using a magnetic stirrer, turning at 300 rpm, in the beakers (Exp. #11–15, Table 2). Stirring the solutions #A and #B greatly modified the morphology of the crystals (see Fig. 2b) and their size was much smaller (1–10 μm scale). They were, moreover, characterized by a much wider range in grain size and by a much higher density of crystals per unit area. Crystals almost covered the entire surface of the immersed vessel walls. Stirred experiments were stopped after 30–60 h. The net mass of precipitated calcite in each experiment is given in Table 2.

3.2. pH and Total Alkalinity of the Precipitating Solution

Solution pH was measured using a pH-meter and a Beckman pH-electrode with temperature compensation. The system pH-meter/electrode was calibrated before each use and repeated pH measurements showed a reproducibility of ± 0.01 pH unit.

We first carried out a series of experiments monitoring the pH as a function of time and of the typical amount of calcite precipitated. It was found for each run that the pH rose rapidly over a time of 10-15 h, after which it leveled off to a nearly constant value where the crystal growth took place. A gradual increase in pH less than 0.02 pH unit/d was still observed in the plateau region. The period during which crystals were allowed to grow was typically 48 h, so that the range of pH variation during an experiment was less than 0.04 pH units (see Fig. 3). However, the final pH value for each experiment was somewhat different. As all experiments were carried out at constant temperature, these differences in pH are not expected to reflect fluctuations in the gaseous/dissolved species equilibrium, but rather reflect changes in the rate of gas supply from the $(NH_4)_2CO_3$ crystals (resulting from varying hydration state of the crystal surfaces of the $(NH_4)_2CO_3$, or from varying transfer rates across the partially clogged fritted filter). It was then possible to carry out growth experiments that gave a wide range in the amount of calcite precipitated, each of them being characterized by different pH values. The values of the pH sampled ranged from 7.98 to 8.40 for the non-stirred solutions, and from 7.65 to 8.22 for the stirred solutions. The results of all experiments are given in Table 2. We note that these differences in pH between each experiment are far outside the uncertainties of the measurement.

The total alkalinity of the precipitating solution was immediately determined after the experiment was stopped by titration using the Gran graphical procedure. Repeated titrations of the total alkalinity carried out by weighing the reagents led to a reproducibility better than 1%. The in-run evolution of the total alkalinity in the solution closely followed that of the corresponding pH. The total alkalinity of the starting $CaCl_2$-NH_4Cl solution was $\sim$0 meq/L and rose after 10–15 h to 11.0–28.9 meq/L for non-stirred and to 5.1–20.2 meq/L for stirred solutions (Table 2).

The actual growth experiments were done during the period indicated by the gray region in Figure 3. As the first calcite crystals were observed after 24–48 h (after the precipitating solutions had reached a quasi-steady state), and considering that combining the pH and the total alkalinity results appear to accurately reveal the solution chemistry, we believe that calcite crystals were grown in stable conditions in each experiment. We will later use both pH and alkalinity values determined at the end of each of the growth experiments as our estimate of the crystal growth conditions.

3.3. Speciation in Solution and the Supersaturation Index

Precipitation of calcite results from the supersaturation of the experimental solution with respect to calcite, as defined in Eqn. 8. In our experiments, the amount of calcium removed from the solution by the precipitation of calcite being always less than 10% of the total Ca, the concentration of calcium in the mother solution is assumed constant during the course of each exper-

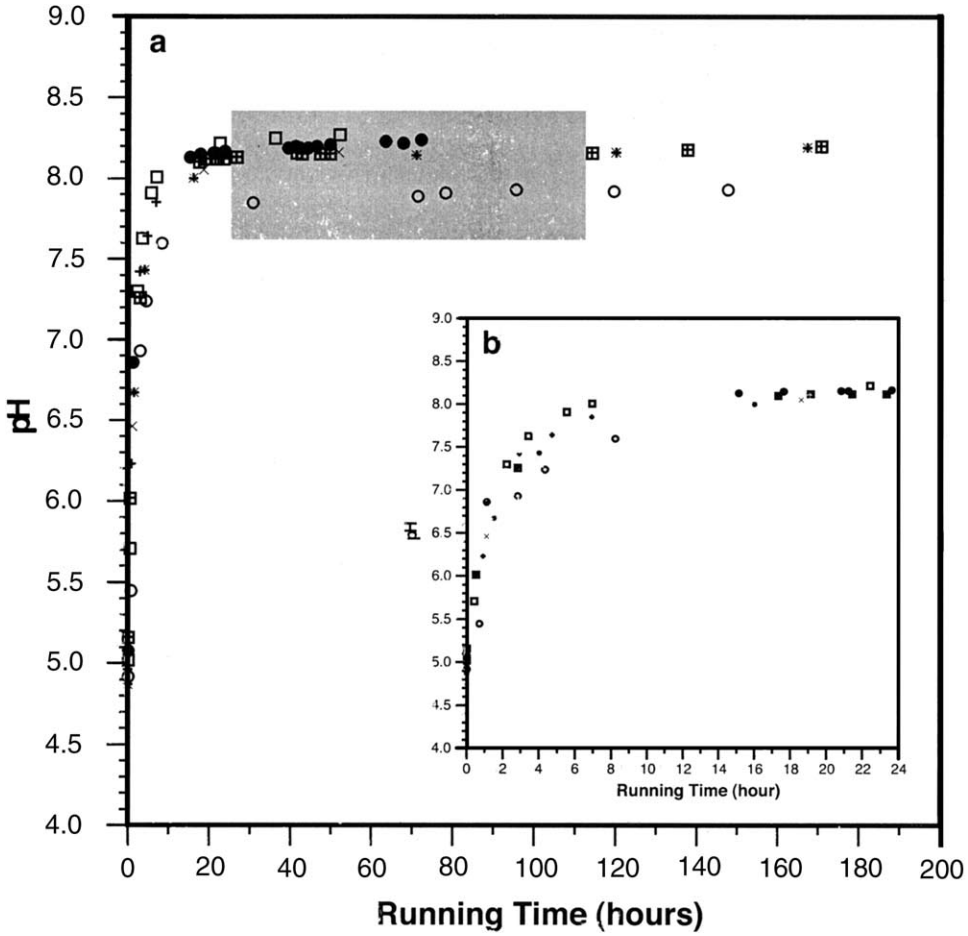

Fig. 3. Graph of pH in the solution versus the time since the system was sealed. The shaded region corresponds to the "plateau" region where the pH for any given run is almost constant. This is the condition where samples were taken. Note that there are distinct values of pH for each run in the plateau region. Each symbol corresponds to a separate run. Graph b) is an enlarged view of pH evolution during the first 24 h of the system.

iment and equal to the original $CaCl_2$ concentration. Therefore, to determine the saturation index of the solution with respect to calcite (represented by Ω), the concentration of the dissolved CO_3^{2-} species in the experimental solutions must be determined. This was calculated using the pH and the total alkalinity values of the precipitating solution. Using the equilibrium reactions (3) and (7), the electroneutrality of the solution and the definition of its total alkalinity, we can reduce the system of equations for CO_3^{2-} to:

$$\left[CO_3^{2-}\right] = \frac{\text{Alk} - \left[NH_3\right]}{2 + \dfrac{\left[H^+\right]}{K_2^*}} \tag{11}$$

with:

$$\left[NH_3\right] = \frac{\left[Cl^-\right] + \text{Alk} - 2\left[Ca^{2+}\right]}{1 + \dfrac{\left[H^+\right]}{K_{NH_3}^*}} \tag{12}$$

where Alk denotes the total alkalinity measured in the solution and corresponds to:

$$\text{Alk} = \left[NH_3\right] + \left[HCO_3^-\right] + 2\left[CO_3^{2-}\right] \tag{13}$$

Calculated $[CO_3^{2-}]$ values are reported in Table 2. They vary by a factor of 5 to 20 for unstirred and stirred solutions (from 60–339 μmol/L and from 13–284 μmol/L) respectively. This range of $[CO_3^{2-}]$ values is similar to those of seawater. Combining calculated $[NH_3]$ values (Eqn. 12) and equilibrium reaction (Eqn. 3), we calculated that the concentration of total nitrogen species did not increase by more than 10% during the course of each experiment. Propagation of the shifts in values in the parameters in Eqns. 11 and (12) demonstrates that the calculated concentration of carbonate ions is highly dependent on the pH as well as on the dissociation constants for both the carbonate (K_2^*) and the ammonium $K_{NH_3}^*$ systems. For decades, a vast number of studies has focused on determination of the dissociation constants of acids in solution and has shown the major influence of temperature and salinity in controlling the speciation. To our knowledge, the most comprehensive study focusing on ammonium dissociation was carried out by Clegg and Whitfield (1995). Their study pointed out the role of the chemical composition of the solution on the dissociation constant of ammonium. Because our solutions are chemically far

from natural samples (high ammonium and calcium concentrations), the ammonium dissociation constants given by them may not be applicable here. Therefore, we determined them experimentally by NaOH titration. The titration was done for the two $CaCl_2$-NH_4Cl mother solutions (#A and #B) and was repeated several times at room temperature to minimize uncertainties. Calculations led to a reproducible value for the ammonium dissociation constant of $pK_{NH_3} = 9.58 \pm 0.01$, identical, within errors, in the two solutions. This value is somewhat different than the value given by Clegg and Whitfield (1995) for a seawater solution ($pK_{NH_3} = 9.34$ at T = 22 °C and S = 38 ppt).

Unfortunately, the same approach cannot be applied to the carbonate system because of the presence of the ammonium system. The second dissociation constant of carbonic acid (K_2^*) was then calculated using the thermodynamical model of Millero (1995). The constants used here are $pK_2 = 9.12$ and $pK_2 = 9.09$, corresponding to solutions #A and #B, respectively. Similarly, the calcite solubility product is a function of temperature and the salinity. We calculated values using the expression developed by Mucci (1983) and determined $pK_{sp}^* = 6.32$ and $pK_{sp}^* = 6.58$, for solutions #A and #B, respectively.

Using the constants discussed above, the saturation indices (Ω) with respect to calcite were calculated for the precipitating solutions (Eqn. 8). The departure from equilibrium (Ω) in each experiment was found to range from 3 ± 1 to 105 ± 23 for unstirred solutions and from 4 ± 1 to 71 ± 11 for stirred solutions. All the experimental solutions were supersaturated with respect to calcite and cover a wide range of supersaturation conditions.

The errors propagated by the dissociation constants and the solubility product of calcite, are assumed to be identical for all the experiments and should not significantly alter trends defined by the data. The errors reported in Table 2 are then estimated from the propagation of the uncertainties in the pH and alkalinity values in each experiment.

3.4. Precipitation Rates

We first note that the total range in duration of the experiments is about a factor of four. In contrast, the amount of Ca removed from the solutions ranges over a factor of 1000. It is thus evident that the precipitation rate is controlled by the chemistry. Several studies have been carried out to determine the rates of calcite crystal growth and the chemical states of the precipitating solutions that govern this growth. Using seed crystals of known surface area, the rates of growth have been measured from different solutions by other researchers. The precipitation rate (represented as R) is given in terms of the growth of the crystal per unit area of the reacting surface (μmol/m^2/h). Extensive studies by Zuddas and Mucci (1994a, 1994b) have shown that, for solutions in which $[Ca^{2+}] >> [CO_3^{2-}]$, the precipitation rate is independent of $[Ca^{2+}]$. These studies showed that R is essentially controlled by $[CO_3^{2-}]$ and that, under conditions far from equilibrium, the following form of an empirical law is a good phenomenological description of the growth rate:

$$\log R = n_2\left(\left[CO_3^{2-}\right]\right) + \log k_f \qquad (14)$$

where k_f is a rate constant and n_2 is the empirical "reaction rate order" (see Zuddas and Mucci, 1994a for more extensive references.)

Intrinsic precipitation rates (Ca deposited/Area of calcite crystals/s) have not been determined in the experiments reported here. Instead we estimated the precipitation rates of each experiment using Eqn. 14 and the empirical values of k_f and n_2 inferred from experiments carried out by Zuddas and Mucci (1994a, 1994b) for NaCl-$CaCl_2$ solutions corresponding to ionic strength, I = 0.55 and I = 0.93 ($n_2 = 2.73$, $\log k_f = 6.07$, and $n_2 = 3.34$, $\log k_f = 6.24$, as best approaching the conditions of solutions #A and #B, respectively). For solutions #A and #B, the calculated log R values range from 1.5 ± 0.7 to 4.7 ± 9.3 μmol/m^2/h for the unstirred solutions, and from −0.1 ± 0.5 to 4.4 ± 0.1 μmol/m^2/h for stirred solutions.

3.5. Δ^{44}Ca of Calcite Crystals

The isotopic compositions (δ^{44}Ca) of calcite crystals were determined in every precipitation experiment. Results are expressed as deviations from the values of δ^{44}Ca in the precipitating solution ($\Delta^{44/40}Ca = \delta^{44}Ca_{crystal} - \delta^{44}Ca_{solution}$, according to Eqn. 10) and are reported in Table 2. For simplicity, we will use $\Delta^{44}Ca = \Delta^{44/40}Ca$. Inspection of the data shows that a wide range in Δ^{44}Ca values was observed (from 0.00 ± 0.12 ‰ to −1.34 ± 0.15 ‰) with crystals being systematically enriched in the light isotope ^{40}Ca compared to the precipitating solution. As a maximum of 10% of total calcium was precipitated, no effect would occur on the parent reservoir that was larger than analytical errors. The variations observed for Δ^{44}Ca in calcite crystals exceed by about one order of magnitude the analytical uncertainties. The Ca isotopic shifts in synthetic calcite were found to cover almost the full range of calcium isotopic shifts measured in calcite and aragonite samples precipitated from seawater as reported by other workers (Skulan et al., 1997; Zhu and Macdougall, 1998; Halicz et al., 1999; Nägler et al., 2000; Gussone et al., 2003).

To test the homogeneity of Δ^{44}Ca in crystals grown in the solution column, calcite crystals attached to the vessel walls were handpicked at different depths and analyzed for calcium isotopes before dissolving the remaining crystals for the bulk Δ^{44}Ca determination. For this exercise, Exp. #2 and #10 (see Table 2) were done and correspond to bulk crystals precipitated from solutions #A and #B, respectively. Hand picked crystals were taken from different layers and analyzed in each of these experiments (see Table 3). There was no difference detected between the bulk samples of an experiment at different depths or the small mass of hand picked crystals compared to the bulk precipitates. Thus, there is no isotopic zoning apparent on a micro or macro scale in these experiments. Results are reported in Table 3. For solution #B (Exp. #10), the number of crystals precipitated per unit area was uniform from the top to the bottom of the vessel walls. In contrast, a clear transition in the concentration and the mean size of the crystals was observed in Exp. #2 (precipitation from solution #A) at ~1 cm below the solution surface. At shallower depth, crystals were larger and more concentrated per unit area than at deeper depth in the solution column. Despite these observations, calcium isotopes in crystals precipitated at different depths in these

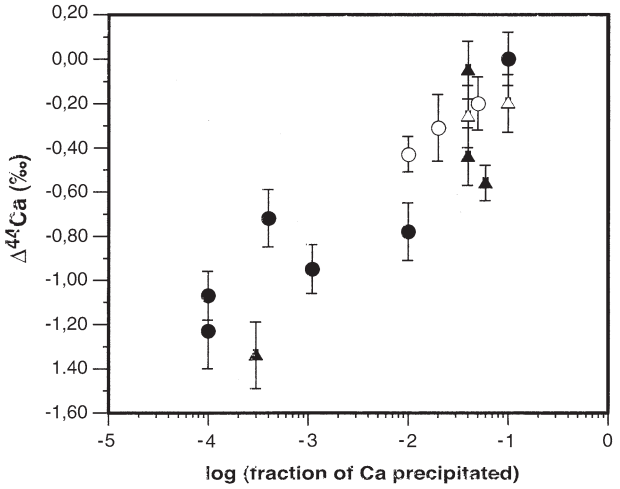

Fig. 4. Graph of $\Delta^{44}Ca$ versus log of the fraction (f) of Ca removed from the solution by crystal growth. There is a systematic trend of $\Delta^{44}Ca$ from low values of f to zero at high values. There is wide dispersion along this trend and no precise correlation except for the stirred solution. Black symbols correspond to experiments during which the precipitating solution was not stirred. Open symbols correspond to experiments during which the precipitating solution was vigorously stirred. Circles correspond to solution #A ([Ca] = 0.15 mol/L); and triangles correspond to solution #B ([Ca] = 0.015 mol/L).

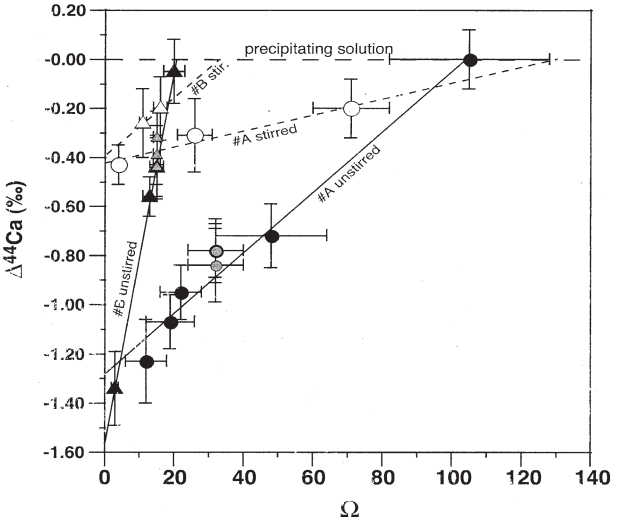

Fig. 5. Comparison of $\Delta^{44}Ca$ between the calcium isotopic composition of calcite crystals relative to that of the precipitating solution versus the supersaturation state of the solution (Ω), Black circles correspond to experiments on solution #A ([Ca] = 0.15 mol/L) during which the precipitating solution was not stirred. Gray circles correspond to crystals handpicked at different depths from the beaker walls in the unstirred solution. Experiments done with solution #B ([Ca] = 0.015 mol/L) are shown as black or grey triangles. The experiments done with stirring are shown as open circles for solution #A and open triangles for solution #B. Note that the data for both of the two unstirred solutions pass through the point $\Delta^{44}Ca = -1.5‰$.

two solutions did not exhibit any shifts. These results showed that neither the chemical stratification of the solution, revealed by the change in the crystal size distribution, nor measurement on a few individual crystals, was associated with resolvable changes in the calcium isotopic abundances in the crystals.

Figure 4 shows the measure $\Delta^{44}Ca$ plotted against the logarithm of the fraction (f) of Ca removed from the solution in each experiment (see column 4, Table 2). The range is from 0.01 to 10% of total Ca removed. There is a well-defined, general correlation of $\Delta^{44}Ca$ with f, the lowest value occurring at very small f. However, this is only a broad relationship and no strong quantitative relationship is observed. The mixed solutions have only small effects. In contrast, the relationship between $\Delta^{44}Ca$ and the supersaturation index with respect to calcite (Ω) is very regular as illustrated in Figure 5. It is shown that the two solutions (#A and #B) behave in similar but distinctive manners. For each of the experimental conditions, lower supersaturation indices were found to be associated with larger Ca isotopic fractionations. This is true for both unstirred and stirred solutions. However, solution #A ([Ca] = 150 mmol/L) has a much lower slope ($\Delta^{44}Ca$ vs Ω) than that for solution #B ([Ca] = 15 mmol/L). The non-stirred solutions at $\Omega = 1$ have an intercept for $\Delta^{44}Ca = -1.5 \pm 0.25‰$. In contrast, the stirred solutions of both solutions #A and #B, the isotopic shifts are much diminished and show distinctive low slopes as compared to the unstirred solutions. For the stirred solutions at the $\Omega = 1$ intercept, corresponding to solutions at equilibrium with calcite, $\Delta^{44}Ca = -0.40 \pm 0.15‰$.

If we plot $\Delta^{44}Ca$ versus $[CO_3^{2-}]$ (Fig. 6), we find that all the data for the unstirred solutions plot on a single line. This is in contrast to the regularities seen in Figure 5 of $\Delta^{44}Ca$ vs Ω where the two solutions lie on different lines. A similar but different "single correlation line" is observed for the stirred solutions (Table 2, Exp. #11-15), but the values define an array with a very low slope. Note that the same behavior is observed when $\Delta^{44}Ca$ is compared to the sum of HCO_3^- and CO_3^{2-}

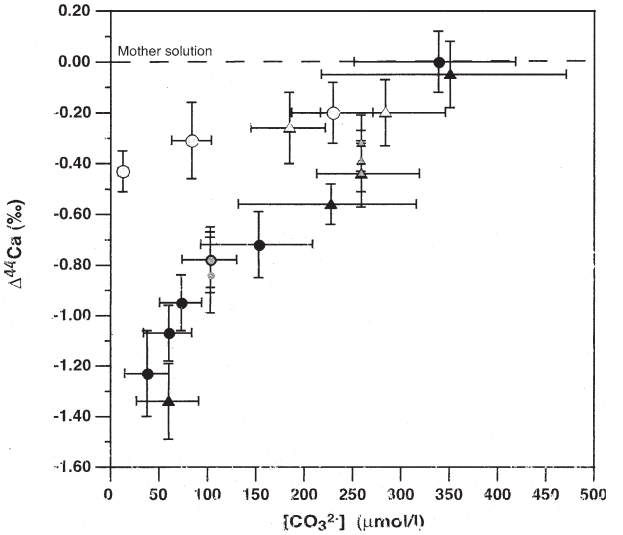

Fig. 6. Graph of $\Delta^{44}Ca$ vs $[CO_3^{2-}]$ for solutions #A and #B. An almost identical display is found if $\Delta^{44}Ca$ is plotted against $[CO_3^{2-}] + [HCO_3^-]$ but with only a shift in the scale for the ordinate. Unstirred solutions are filled circles or triangles. Open circles are for stirred solutions. Again, note the clear difference between unstirred and stirred solutions. However, in this representation, there is no difference between the two solutions (#A and #B) for the unstirred data (see Fig. 5).

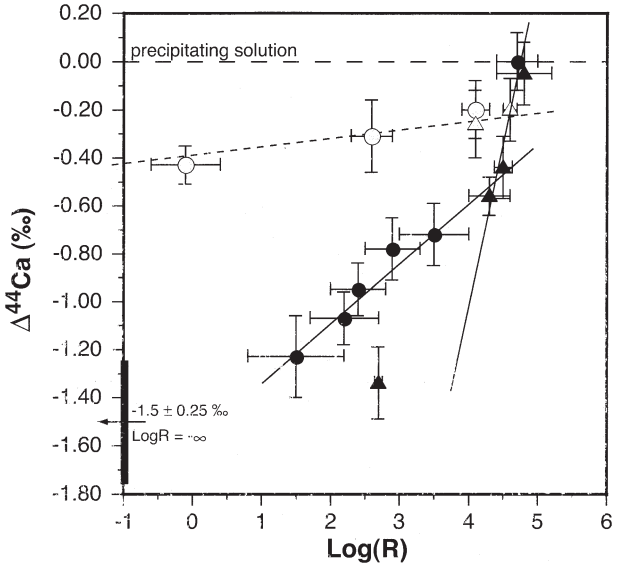

Fig. 7. Graph of Δ^{44}Ca vs log R where R is the rate of crystal growth. Using the empirical relationship between R and Ω (see Eqn. 14, section 3.4): filled circles (#A) and triangles (#B) represent data from unstirred solutions. Open symbols are from stirred solutions. There is an apparent change in behavior at large R (log R > 4) (see line through selected data). There should be a change in behavior at very low R values.

species as the ratio CO_3^{2-}/HCO_3^- is rather constant. In all representations, it is clear that there are distinctive trends corresponding to stirred and unstirred conditions. These results show that the carbonate species (either $[HCO_3^-]$, $[CO_3^{2-}]$ or a mixture of them), are the controlling species in both the calcite precipitation and the isotopic fractionation.

Variations of Δ^{44}Ca are compared to the calculated precipitation rates in Figure 7. For the unstirred solutions of #A and #B, Δ^{44}Ca appears to regularly increase with increasing log R in the interval $1 < \log R < 4$. For higher growth rates when $\log R > 4$, Δ^{44}Ca tends to depart from a simple linear relationship and indicates changes in behavior at the high precipitation rates. Finally, based on the relationship between Δ^{44}Ca vs Ω reported in Figure 5, we expected that the largest Δ^{44}Ca (-1.50 ± 0.25‰) should be observed at the $\Omega = 1$ condition, which would correspond to equilibrium between solution and calcite. The $\Omega = 1$ condition is characterized by an infinitely slow precipitation rate ($\log R = -\infty$). In that case, for $\log R < 1$, changes in the precipitation rate should not affect Δ^{44}Ca if there is an "equilibrium" fractionation ($\Delta^{44}Ca = -1.5 \pm 0.25$‰ at $\log R = -\infty$). The lowest rate we measured corresponds to $\log R = 1.5$ with the value of $\Delta^{44}Ca = -1.23 \pm 0.17$‰. We estimate that this would correspond to $\Delta^{44}Ca = -1.5 \pm 0.25$‰ at infinitely slow rates. It is certainly possible that the true equilibrium effect is somewhat larger than this and is somewhat suppressed by some supersaturation precipitation as we did not reach the $\Omega = 1$ condition.

For the stirred solutions, it is observed that the precipitation rates have very little effect. The values of Δ^{44}Ca for the stirred solutions are clearly depressed by roughly ~0.2 per mil relative to the bulk solution. This is in sharp contrast to the large regular increase observed under unstirred conditions.

4. DISCUSSION

4.1. Incorporation of Calcium Isotopes into the Calcite Lattice

The results of the experiments presented in this study demonstrate that a clear isotopic fractionation occurs during the incorporation of calcium into the calcite lattice and that the effects are, to a large extent, controlled by the precipitation rate. We propose that the partition of calcium isotopes between the precipitating solution and growing crystals reflects equilibrium exchanges, which are more or less affected by kinetics effects depending on how fast the crystals grow.

The experimental conditions of stirring or of not stirring the solution greatly affect the calcium isotopic composition of calcite crystals and show that the transfer of reactants from the bulk solution to the surface of the crystals is the limiting mechanism during crystal growth (e.g., (Nielsen and Toft, 1984). Furthermore, the results taken under the experimental conditions reported here show that the supply of carbonate species controls the calcite precipitation rate and thus is carbonate "transport limited." We conclude that, under our experimental conditions, the calcite precipitation rate is controlled by the supply of carbonate species from the bulk solution to the surface of the growing crystals and that the supply of Ca from the bulk solution does not limit the rate of crystal growth. The largest Ca isotopic effect is found for the slowest precipitation rate with no stirring and the value reached is the same at the very different [Ca] levels used. In all cases, in our experiments, $[Ca^{2+}] >> [CO_3^{2-}] + [HCO_3^-]$.

With regard to the equilibrium fractionation factor for Ca isotopes between calcite crystals and solution, there are no theoretical models yet available. Kinetic effects due to the rate of Ca^{2+} ion diffusion at the crystal-liquid interface would suggest that large isotopic shifts should occur for small amounts of crystal growth (see 4.2). Using the square root of the ratios of the masses $\sqrt{44/40}$ as estimates of the relative velocities, it would be expected that very large kinetic effects would be observed. These have not been found either by previous investigators or in the present work. For the observed effects of the order of 1‰ to be attributed to the effective mass of diffusing hydrated Ca^{2+} complexes would require their masses to be ~1000 amu. This has been proposed by Gussone et al. (2003) as a possible explanation. However, such an enormous hydration sphere does not appear plausible to us as the typical first hydration sphere is 6–10 molecules.

In considering the results of the present work, it can be seen that the controlling factor is the supply of CO_3^{2-} and HCO_3^- to the growing crystal interface. As the exchange rate between these two species is rapid, there should be a parallel relationship (see Eqn. 7) between their concentrations in this matter. The rate of growth in a solution with $[Ca^{2+}] >> [CO_3^{2-}]$ clearly always provides a large abundance of Ca^{2+} at the interface and in the solution, and a diffusion limited supply of CO_3^{2-} and HCO_3^- at the interface with the crystal. We here assume that there is, in fact, an equilibrium fractionation factor for Ca between the crystal and the solution of $\Delta^{44}Ca \approx -1.5$‰. In this case, the observed fractionation in the growing crystal will depend on how rapidly Ca ions can precipitate in a surface region thicker than the equilibrium zone at the growing inter-

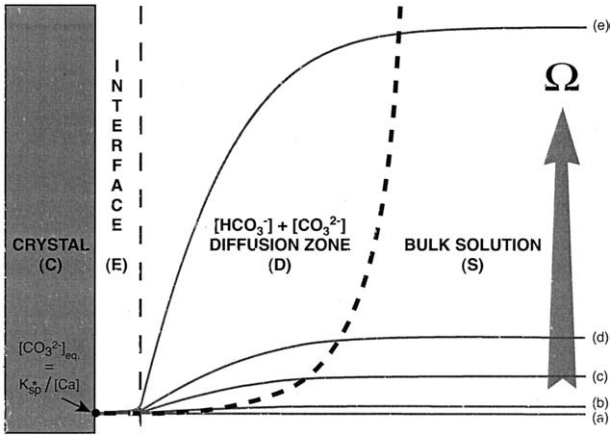

Fig. 8. A schematic diagram showing the calcite crystal (C); the narrow interface (E) where crystal and surface boundary layer are in chemical and isotopic equilibrium through exchange reactions; the diffusive zone (D) where carbonate ions have diffused in at higher than saturation concentrations; and, the exterior solution (S). the curves show the values of supersaturation (driven by $[CO_3^{2-}]$) as a function of the position away from the interface. Curve (a) is at saturation; curves (b), (c), (d) and (e) show increasing penetration of high Ω concentrations into region (D). In the diffusive region, all CO_3^{2-} is precipitated if $\Omega > 1$. The larger the area under the curve, the larger is the amount of Ca that is precipitated and the closer to the solution value is the calcium isotopic composition of the crystal. Stirring or convection decreases the distance over which diffusive carbonate flow into the region (D) takes place.

face relative to the rate of exchange for the thin surface layer necessary to achieve isotopic equilibrium (see Fig. 8). If the isotopic exchange rate is small compared to the precipitation rate (as is certainly the case in most of the experiments if one considers the values of log Ω), then the crystal will grow because of the removal of Ca^{2+} and CO_3^{2-} from the zone of supersaturation. The larger the contribution of Ca from the supersaturation zone is, the lower will be the isotopic shift in the crystal relative to the fluid. Ultimately, at very fast precipitation rates, all Ca will be removed from the bulk solution and not just from the thin equilibrium interface region. Then, no isotopic effect should be observed.

If the solution is stirred, then the effective thickness of the boundary layer (region (E) is decreased (i.e., better mixed with the mother solution) and a zone of high CO_3^{2-} is brought closer to the equilibrium interface providing a higher concentration gradient of CO_3^{2-}. This ultimately leads to removing more Ca from the bulk solution without fractionation. Such a condition is not actually achieved in our experiments but appears to be approached with the stirring method used. In cases without stirring, the rate limiting effect is the diffusive inflow of CO_3^{2-} and HCO_3^-. This rate should increase proportionately to Ω and the inverse thickness of the boundary layer.

This model requires that there is an equilibrium fractionation factor for Ca isotopes at the level of $\sim$1.5‰ for 4 amu. Explicit experimental tests must be done and theoretical models need to be explored to evaluate the true equilibrium characteristics. The approach presented here follows some of the earlier models of calcite growth (Ohara and Reid, 1973; Turner, 1982; Nielsen, 1984). The actual state of the interface during calcite growth has been studied by several groups. With regard to the Ca atoms-ions at the equilibrium interface, Cicerone (1992) has argued that the surface has adsorbed Ca^{2+} ions under the pH conditions used here. This creates a net positive charge and facilitates the incorporation of CO_3^{2-} ions into the crystal surface with concurrent growth. Whether or not CO_3^{2-} or HCO_3^- is the dominating species governing growth is not clear. Insofar as the exchange rate between these two species is very rapid, then the resultant growth will not be affected.

In the results presented here there is a remarkable regularity shown in Figures 5 and 6 that merits comment. Note that in Figure 5 the ratio of the slopes for the unstirred solution #B compared to #A is $\sim$5. Similarly, the ratio of the slopes for the same stirred solutions is $\sim$4. This difference in slopes is not distinguishable considering the uncertainties. Further, the end points at $\Omega = 1$ are the same for both the unstirred solutions and a distinctly different end point is found for the two stirred solutions. Further, in Figure 6, we see that both solutions #A and #B are on the same correlative line versus $[CO_3^{2-}]$ for each case. This is in sharp contrast to the different line found in the Ω representation in Figure 5.

The presence of a significant effect on $\Delta^{44}Ca$ for stirred solutions requires attention. It is obvious that if the distance between the crystal-liquid interface boundary and the undepleted solution is decreased by stirring, then the diffusion inflow of CO_3^{2-} ions would be enhanced by the inverse scaling factor of the distances (see Fig. 8). This would then increase the amount of Ca^{2+} ions precipitating from outside the "equilibration zone" (E) and decrease the isotopic effect. The magnitude of this effect should increase proportionally to Ω. To explain why the apparently limiting value of $\Delta^{44}Ca_{stirred} = \sim 0.4‰$ is reached is not obvious. These observations require a quantitative explanation. In addition, we note that the solutions differ by a factor of 10 in $[Ca^{2+}]$ concentrations, whereas the difference in slopes shown in Figure 5 is $\sim$5 as outlined in the previous paragraph for the unstirred solutions. Offhand, one would expect the ratio of the slopes to be a factor of 10. However, if the salinity effects on the equilibrium constants, as discussed in Section 3.2, are taken into account then the factor should be $\sim$6 from the ratio of the Ω values which is close to the observed slope. It appears that even this numerical relationship is compatible with the model outlined above.

Using the empirical law for the precipitation rate, we infer that to achieve the Ca isotopic composition of calcite to be in equilibrium with the solution requires that the precipitation rate not exceed 10 μmol/cm^2/h. For faster precipitation rates, kinetic effects will apply driving Ca isotopic composition of calcite toward the bulk solution value ($\Delta^{44}Ca = 0‰$). The design of the experiments presented here is rather simple and not well directed toward exposing the detailed growth history of the crystals. The experiment allows CO_2 and NH_3 and associated species to diffuse from the atmosphere into the solution. As a result, the time evolution of the concentration of these species at a given position requires its own analysis. The crystal growth then involves transport mechanisms at the crystal-liquid interface considering the time evolution of the local medium that depends on diffusive inflow from the gas-liquid interface. In the case of stirring, then the diffusion across the gas-liquid interface (coupled with enhanced transport at the surface from stirring) is then homogenized throughout the volume of the solution. This is in contrast to the unstirred case.

The concentration of these "gaseous" species is now the volume average of the inflow from the liquid-gas interface. This then evolves differently with time as compared to no stirring where there is a diffusion gradient as a function of depth in the solution in the beaker. As a result, it is not possible to provide a simple analysis of the crystal growth and isotopic fractionation that permits more detailed comparison. We note that in a detailed study of Fe elution with an ion exchange resin that the magnitude of the Fe isotopic fractionation was found to increase as the elution rate decreases (Roe et al. 2003). These workers inferred that this provided strong evidence for an equilibrium isotopic fractionation that is diminished due to kinetic complications during rapid elution. It seems clear from that report and the present study on Ca that equilibrium isotopic fractionation may be a determining factor and that sometimes kinetics effects can alter the results by subduing the equilibrium effects.

4.2. The Role of Temperature and pH

Investigation of Ca isotopic compositions in calcite and aragonite have led to the recognition that there is a temperature effect shifting the isotopic composition between solution and precipitated carbonates (De La Rocha and DePaolo, 2000; Nägler et al., 2000; Gussone et al., 2003). Various Δ^{44}Ca vs T relationships have been observed ranging from 0.25‰/°C down to 0.015‰/°C. This has led to the suggestion that the Ca isotopic compositions of carbonates may serve as a seawater paleothermometer. Recently, Gussone et al. (2003) proposed a model of Ca isotope incorporation into carbonates which involves diffusion at the solid/liquid interface of Ca^{2+}-aqua-complexes ($Ca[H_2O]^{2+}$ $\bullet mH_2O$) of mass 520–640 amu with some unspecified temperature dependent fractionation mechanism. As argued above, we propose that it is the competition between the equilibrium fractionation factor and the precipitation rate due to supersaturation near the interface by diffusive inflow of CO_3^{2-} ions that governs the behavior, not kinetic isotopic fractionation of Ca species. In a model dependent on Ca isotopic diffusion, it is expected that the initial diffusion growth would give isotopic effects bounded by the relative fluxes of species $\sqrt{m_1/m_2}$ assuming a simple mass-velocity dependence, or more plausibly, from solution $\sqrt{D_2/D_1}$ (considering the ratio of the fluxes at the boundary, flux $= -D\nabla C$) for species of mass m_1 and m_2 leading to a value of $\left(m_1/m_2\right)^{1/4}$ (here, $(44/40)^{1/4} \approx 1{,}024$) if the ratio of the diffusion constants goes like $\sqrt{m_1/m_2}$. Even in the crystals grown at the slowest rate, where only 0.01% of the Ca in solution was removed (see Table 2 and Fig. 4), the results show $\Delta^{44}Ca = -1.23$‰, that is ~20 times smaller than expected by a Ca diffusion model. Estimates of hydration complexes of Ca in aqueous solution of mass ~600 amu appear far too large to be plausible. The relationships observed in this work clearly show that CO_3^{2-} diffusion is the governing mechanism for calcite growth. This is precisely what should be expected from solutions where $[Ca^{2+}] >> [CO_3^{2-}]$ or $[Ca^{2+}] >> [CO_3^{2-}] + [HCO_3^-]$. Here, we have proposed an alternative model in which temperature effects on Δ^{44}Ca shifts are caused by their influence on the equilibrium constants.

Temperature may affect Δ^{44}Ca by its influence on the dissociation constants of carbonic acid in solution by enhancing or diminishing the extent of precipitation from regions of supersaturation near the crystal-liquid interface. No supersaturation should give the equilibrium value. In other words, changes in temperature will modify the relative proportions of the carbonate species in solution (H_2CO_3, HCO_3^- and CO_3^{2-}) and will then change the saturation state of the solution (Millero, 1995) and thus increase/decrease the Ca precipitated out of isotopic equilibrium. As most natural solutions meet the condition $[Ca] >> [CO_3^{2-}]$ so the supply of carbonate species is the rate limiting parameter. The actual temperature dependence of the hypothecated equilibrium fractionation factor proposed here will have to be explored both experimentally and theoretically using the methods of statistical mechanics with consideration of the partition functions in conjunction with refined spectroscopic data on Ca complexes in crystals and in solution.

In the model proposed here, we assume that growth from a narrow equilibrium boundary layer, coupled with diffusive $[CO_3^{2-}]$ inflow from a larger region with $\Omega > 1$, that dumps bulk unfractionated Ca from larger domains of the fluid into the growing crystal-liquid interface. Using the extensive study of the thermodynamics of carbon dioxide in sea water (Millero, 1995), we have calculated the effects of temperature, salinity and pH for Δ^{44}Ca precipitated from sea water. For our model, these calculations predict that the relationship between Δ^{44}Ca and pH in sea water should be as shown in Figure 9a. Here, we have calculated Δ^{44}Ca as a function of pH assuming the relationship $\Delta^{44}Ca = Q\bullet[CO_3^{2-}]$, where the constant Q is derived from Figure 6. The shifts in Δ^{44}Ca become zero at pH $\geq$ 8.7. The slope of Δ^{44}Ca vs pH is ~1.14‰/pH unit at pH 8–8.4. If we now determine the change in Δ^{44}Ca at pH = 8.2 as a function of temperature using the known behavior of the equilibrium constants, it is found that the slope is 0.02‰/°C (Fig. 9b). This is in accord with the estimate of the temperature effect found by Gussone et al. (2003). The sensitivity of Δ^{44}Ca with regard to changes in salinity is also shown in Figure 9b, with the ordinate scale shown at the top.

From these considerations it appears that the model of diffusion-limited carbonate input is in general agreement with the available data. It then relegates the paleotemperature aspects to the effects on the equilibrium constants of hydrated CO_2 species, and is not just an intrinsic isotope effect of Ca. This may still be of some value although the problem of convective processes near the interface must always be considered.

At this stage, the nature of carbonate species actually involved in the precipitation of calcite should be discussed as no consensus has been reached. Zuddas and Mucci, (1994a) suggested that both HCO_3^- and CO_3^{2-} are involved in the precipitation of calcite from strong electrolyte solutions but that the precipitation rate depends on the cube of $[CO_3^{2-}]$ and on the square of $[HCO_3^-]$. As a result, the net precipitation rate appears dominated by the reaction involving CO_3^{2-} at the expense of reactions involving HCO_3^-, for pCO_2 not exceeding 3×10^4 Pa. This condition applies in all our experiments, for which a maximum of $pCO_2 = 200$ Pa is calculated if equilibrium is assumed for the atmosphere/solution system. According to their study, only $[CO_3^{2-}]$ can be considered to correctly describe calcite precipitation rates. However, investigation of oxygen isotopes in foraminiferal calcite leads to the interpretation that both of the carbonate species are involved in the calcite precipitation in proportion to their relative contribution to

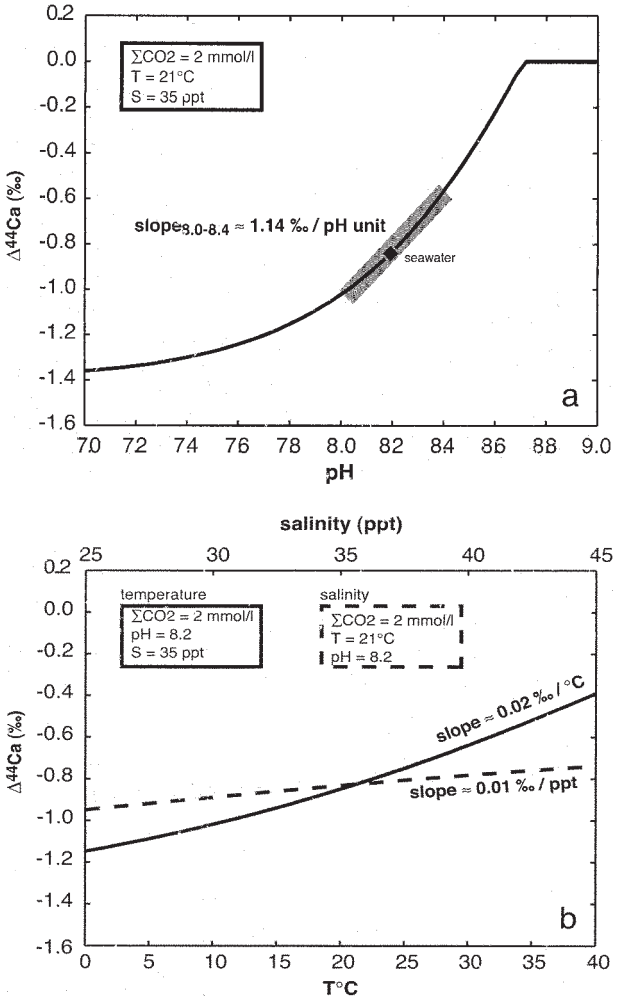

Fig. 9. Graph of $\Delta^{44}Ca$ versus pH for seawater assuming the model of an interface at equilibrium coupled with diffusive transport of CO_3^{2-} toward the interface causing precipitation of bulk Ca from the solution. Here it is explicitly assumed that the relationship between $\Delta^{44}Ca$ and Ω as measured in this report is applicable to seawater. Not the sensitivity to pH; b) The calculated dependence of $\Delta^{44}Ca$ on temperature for seawater assuming the above model. The slope is ~0.02 per mil/°C. A similar calculation for the dependence on salinity is shown by the dashed curve using the upper scale.

the total dissolved carbon (Zeebe, 1999). In this case, precipitation of calcite in our experiments should result from a large contribution of HCO_3^-. In our experiments, $\Delta^{44}Ca$ correlates both with $[CO_3^{2-}]$ and with $[CO_3^{2-}] + [HCO_3^-]$, and we are not able to decipher which scenario applies. Insofar as the reaction rates between CO_3^{2-} and HCO_3^- are rapid, there will not be a distinction. However, this may not prevent effects in C and O isotopes to occur (cf. Turner, 1982).

4.3. Comparison with Previous Studies

We can not explicitly compare our results with the extensive results obtained by Gussone et al. (2003). Their experiment on aragonite precipitation shows $\Delta^{44}Ca = -1.63‰$ at 20°C and a temperature (T) dependence of $\frac{d\Delta^{44}Ca}{dT} = 0.015 - 0.019‰/°C$. The values obtained by us at 20 °C for very small fractional amounts of Ca removal from solution as calcite, and more significantly, for $\Omega \approx 1$ is $\Delta^{44}Ca = -1.5 \pm 0.25‰$. We also find that the temperature dependence due to changes in the equilibrium "constants" is 0.02‰/°C. These results for calcite are in very good agreement with the values found by Gussone et al. (2003). However, we cannot compare the Ω values appropriate for the experiments by Gussone et al. (2003) with the model proposed here as the chemical parameters applicable to their study are not available. The very different behavior of the biogenic precipitates by Nägler et al. (2000) and by Gussone et al. (2003) are not directly explained by the model proposed here. We do not yet have any means of assessing the value of Ω pertinent to the different biologic precipitates, or of the specific reaction paths in organisms. The data on O. universa can be explained by high values of Ω during precipitation. The data on G. sacculifer with some data giving $\Delta^{44}Ca = -3.0‰$ would require that for this organism, there is a two-stage or complex reaction path involved in process. The low values of $-2.6‰$ in some coccolith oozes (Zhu and Macdougall, 1998) and of one sample of G. sacculifer with $\Delta^{44}Ca = -3.3‰$ can not be readily explained by our model. The very large temperature dependence of $\Delta^{44}Ca = 0.25‰/°C$ found in growing G. sacculifer is very difficult to explain in any case.

In so far as the postulated equilibrium fractionation factor for calcite from the present work and the value of $\Delta^{44}Ca$ (20 °C) obtained by Gussone et al. (2003) for aragonite are almost identical, it is suggested that the equilibrium value for both phases is about the same. We further note that the fractionation between bone (phosphate) and body fluid in vertebrates is $\sim -1.5‰$ (Skulan and DePaolo, 1999). The typical value of carbonates precipitated in deep sea environments is $\Delta^{44}Ca \sim -1.5‰$ (Zhu and Macdougall, 1998). However, there is a considerable range observed (-0.8 to $-3.0‰$). Overall, it appears that a strong circumstantial case can be made for equilibrium fractionation of about $-1.5‰$ as the key process. It is possible that the true value is somewhat higher as we can not argue that our experiment has no extra precipitation from solution. However, if high values of Ω can be maintained at the site of crystal growth (whether in an inorganic system or by an organism), then the equilibrium value will be partially suppressed or completely cancelled.

5. CONCLUSION

It is found that there is a regular behavior of the isotopic shifts of ($\Delta^{44}Ca$) in calcite crystals compared to that of the mother solution. This is directly dependent on $[CO_3^{2-}]$ or on the degree of oversaturation (Ω). Solutions with [Ca] of 150 mmol/L and 15 mmol/L both show analogous behavior with a value of $\Delta^{44}Ca \sim 1.4‰$ for $\Omega \approx 1$ and a regular decrease of this effect toward $\Delta^{44}Ca = 0$ for higher values of Ω. The difference in behavior of $\Delta^{44}Ca$ vs Ω for the two solutions is shown quantitatively to be the result of the shift in the concentration of CO_3^{2-} required for the corresponding dif-

ferences in Ca concentrations. The value of $\Delta^{44}Ca \sim -1.4‰$ for $\Omega \sim 1$ is interpreted as an equilibrium fractionation factor between the calcite crystal and the solution in our experimental conditions. It is shown that the diffusive inflow of $[CO_3^{2-}]$ and $[HCO_3^-]$ to the crystal liquid interface causes crystal growth to proceed with an increasing amount of precipitation of Ca with the isotopic composition of the bulk fluid. The resulting isotopic shifts are thus interpreted to be a mixture of the equilibrium value with the bulk value of the solution. We conclude that, in the system studied, the governing factor controlling the isotopic shift is the oversaturation of a region of the boundary layer by diffusive inflow of CO_3^{2-} and HCO_3^-. These effects are not due to the complex behavior of Ca isotopic fractionation as Ca plays a rather passive role for systems when $[Ca] >> [CO_3^{2-}] + [HCO_3^-]$. The role of temperature is argued to be the result of changes in the equilibrium constants with temperature that enhances or decreases the degree of supersaturation and not just to intrinsic changes in the Ca isotopic fractionation factor.

The experiments reported here exhibit a clear and regular behavior depending on the chemical state of the system and the degree of convective mixing. A generation of experiments under much more tightly controlled physical conditions are now needed so that the detailed mechanism can be better exposed and the model tested. In particular, experiments under more tightly controlled systems where the pH and $[CO_3^{2-}]$ of the solution are close to $\Omega = 1$ and are constant in time. This should directly approach equilibrium conditions, distinct from the approach taken here. The detailed dynamics of calcite and aragonite growth, taking into account the molecular species involved, is important. This matter has received considerable attention for C and O isotopic fractionation which is fundamental to paleothermometry. We note that the excellent experimental and theoretical study by Turner (1982) has given a thorough analysis of the contributing carbon molecules during crystal growth with consideration of the interactions and mechanisms at the growth surface. It would be of value to combine such approaches with Ca isotopic analyses so that the claim of equilibrium effects for Ca could also be compared with the equilibrium values and kinetic effects on the C and O isotopes.

For future experiments we consider that the first and most important effort be directed toward controlled crystal growth at $\Omega \approx 1$, under different pH and temperature conditions and with the thermodynamic parameters determining Ω known. These results would test the hypothecated equilibrium value and inferred temperature dependence of the "K" values. In the present work, we did not do experiments at $\Omega \approx 1$. Possible experimental approaches such as those used by Gussone et al. (2003) close to $\Omega \approx 1$ and with determination of the explicit thermodynamic parameters should lead to a clearer definition of the problem. Once it is established that an equilibrium fractionation factor is indeed the important parameter, then it would be of considerable interest to explore C, O and Ca fractionation patterns under equilibrium conditions and with departures from equilibrium. This has earlier received great attention by some workers who have considered the many different species in carbonate formation from solution. A new look might be of considerable merit.

The attribution of observed isotopic fractionation effects between crystals and fluids solely to kinetic processes is not generally appropriate. The role of equilibrium fractionation must be considered as one of the causal agents. Kinetic effect may sometimes be causal and sometimes simply subdue the equilibrium effects. Without attention to both aspects of the isotopic fractionation processes, the observations can be inadequately interpreted.

In general, we consider that approaching the fractionation of Ca isotopes as a problem in physical chemistry will help bring this interesting research area into a better defined focus with a chance of understanding the so-called "biogenic" effects.

Acknowledgments—This work was supported by DOE DE-FG03–88ER13851. Caltech Contribution #8908(1110). We wish to thank J. Adkins and P. Zuddas for helpful discussions on aspects of aquatic chemistry and crystal growth mechanisms and H. Ngo and J. Chen for their aid in analytical chemistry and spectrometry. A conversation at dinner with Rudi Marcus was very valuable. We thank the reviewers for their constructive comments and questions, particularly one reviewer who meticulously studied the manuscript. The judgment of "nihil obstat" by Jim Morgan, was greatly appreciated

Associate editor: Y. Amelin

REFERENCES

Botttinga Y. (1968) Calculation of fractionation factors for carbon and oxygen isotopic exchange in the system calcite-carbon dioxide-water. *J. Phys. Chem.* **72,** 800–808.

Cicerone D. S., Regazzoni A. E. and Blesa M. A. (1992) Electrokinetic properties of the calcite/water interface in the presence of magnesium and organic matter. *J. Colloid. Interface Sci.* **154,** 423–433.

Clegg S. L. and Whitfield M. (1995) A chemical model of seawater including dissolved ammonia and the stochiometric dissociation constant of ammonia in estuarine water and seawater from −2 to 40°C. *Geochim. Cosmochim. Acta* **59,** 2403–2421.

De La Rocha C. L. and DePaolo D. J. (2000) Isotopic evidence for variations in the marine calcium cycle over the Cenozoic. *Science* **289,** 1176–1178.

Grossman E. L. and Ku T. L. (1986) Oxygen and carbon isotope fractionation in biogenic aragonite: temperature effects. *Chem. Geol.* **59,** 59–74.

Gruzensky P. M (1967) Growth of calcite crystals. In *Crystal Growth, Conference Proceedings of the International Conference on Crystal Growth (1966: Boston MA)* (ed. H. Steffen Peiser), Supplement to *Journal of Physics and Chemistry of Solids* S: **365** Suppl. 1. Pergamon Press, New York.

Gussone N., Eisenhauer A., Heuser A., Dietzel M., Bock B., Böhm F., Spero H. J., Lea D., Bijma J. and Nägler T. (2003) Model of kinetic effects on calcium isotope fractionation ($\delta^{44}Ca$) in inorganic aragonite and cultured planktonic foraminifera. *Geochim. Cosmochim. Acta* **67,** 1375–1382.

Halicz L., Galy A., Belshaw N. S. and O'Nions R. K. (1999) High-precision measurement of calcium isotopes in carbonates and related materials by multiple collector inductively coupled plasma mass spectrometry (MC-ICP-MS). *J. Anal. Atom. Spect.* **14,** 1835–1838.

Hemming N. G., Reeder R. J. and Hanson G. N. (1995) Mineral-fluid and isotopic fractionation of boron in synthetic calcium carbonate. *Geochim. Cosmochim. Acta* **59,** 371–379.

Jiménez-Lopez C., Caballero E., Huertas F. J. and Romanek C. S. (2001) Chemical, mineralogical and isotope behavior, and phase transformation during the precipitation of calcium carbonate minerals from intermediate ionic solution at 25°C. *Geochim. Cosmochim. Acta* **65,** 3219–3231.

Kim S.-T. and O'Neil J. R. (1997) Equilibrium and nonequilibrium oxygen isotope effects in synthetic carbonates. *Geochim. Cosmochim. Acta* **61,** 3461–3475.

McConnaughey T. (1988) ^{13}C and ^{18}O isotopic disequilibrium in biological carbonates: II in vitro simulation of kinetic isotope effects. *Geochim. Cosmochim. Acta* **53,** 163–171.

Millero F. J. (1995) Thermodynamics of the carbon dioxide system in the oceans. *Geochim. Cosmochim. Acta* **59,** 661–677.

Mucci A. (1983) The solubility of calcite and aragonite in seawater at various salinities, temperatures, and one atmosphere total pressure. *Am. J. Sci.* **283,** 780–799.

Nägler T., Eisenhauer A., Müller A., Hemleben C. and Kramers J. (2000) The d44Ca-temperature calibration on fossil and cultured Globigerinoides sacculifer: new tool for reconstruction of past sea surface temperatures. *Geochem. Geophys. Geosyst.* **1(2000GC000091)**.

Nielsen A. E. (1984) Electrolyte crystal growth mechanisms. *J. Crystal Growth* **67,** 289–310.

Nielsen A. E. and Toft J. M. (1984) Electrolyte crystal growth kinetics. *J. Crystal Growth* **67,** 278–288.

Ohara M. and Reid R. C. (1973) Modeling crystal growth rates from solution. Prentice Hall, Englewood, NJ.

Paquette J. and Reeder R. J. (1990) New type of compositional zoning in calcite: insights into crystal-growth mechanisms. *Geology* **18,** 1244–1247.

Plummer L. N. and Busenberg E. (1982) The solubilities of calcite, aragonite and vaterite in CO_2-H_2O solutions between 0 and 90°C, and an evaluation of the aqueous model for the system $CaCO_3$-CO_2-H_2O. *Geochim. Cosmochim. Acta* **46,** 1011–1040.

Plummer L. N., Wigley T. M. L. and Parkhurst D. L. (1978) The kinetics of calcite dissolution in CO_2-water system at 5°C to 60°C and 0.0 to 1.0 atm CO_2. *Am. J. Sci.* **278,** 179–216.

Roe J. E., Anbar A. D. and Barling J. (2003) Nonbiological fractionation of Fe isotopes: evidence of an equilibrium effect. *Chem. Geol.* **195,** 69–85.

Romanek C. S., Grossman E. L. and Morse J. W. (1991) Carbon isotopic fractionation in synthetic aragonite and calcite: effects of temperature and precipitation rate. *Geochim. Cosmochim. Acta* **56,** 419–430.

Russell W. A., Papanastassiou D. A., and Tombrello T. A. (1978) Ca isotope fractionation on the Earth and other solar system materials. *Geochim. Cosmochim. Acta* **42,** 1075–1090.

Schmitt A.-D., Chabaux F. and Stille P. (2003) The calcium riverine and hydrothermal isotopic fluxes and the oceanic calcium mass balance. *Earth Planet. Sci. Lett.* **213,** 503–518.

Skulan J. and De Paolo D. J. (1999) Calcium isotope fractionation between soft and mineralized tissues as a monitor of calcium use in vertebrates. *Proceedings of the National Academy of Sciences* **96,** (*13*), 709–713.

Skulan J., DePaolo D. J. and Owens T. L. (1997) Biological control of calcium isotopic abundances in the global calcium cycle. *Geochim. Cosmochim. Acta* **161,** 2505–2510.

Turner J. V. (1982) Kinetic fractionation of carbon-13 during calcium carbonate precipitation. *Geochim. Cosmochim. Acta* **46,** 1183–1191.

Wasserburg G. J., Papanastassiou D. A., Nenow E. V. and Bauman C. A. (1969) A programmable magnetic field mass spectrometer with on-line data processing. *Rev. Sci. Instr.* **40,** 288–295.

Zeebe R. (1999) An explanation of the effect of seawater carbonate concentration on foraminiferal oxygen isotopes. *Geochim. Cosmochim. Acta* **63,** 2001–2007.

Zhu P. and Macdougall J. D. (1998) Calcium isotopes in the marine environment and the oceanic calcium cycle. *Geochim. Cosmochim. Acta* **62,** 1691–1698.

Zuddas P. and Mucci A. (1994a) Kinetics of calcite precipitation from seawater: I. A classical chemical kinetics description for strong electrolyte solutions *Geochim. Cosmochim. Acta* **58,** 4353–4362.

Zuddas P. and Mucci A. (1994b) Kinetics of calcite precipitation from seawater: II. The influence of the ionic strength *Geochim. Cosmochim. Acta* **62,** 757–766.